Resonant tuning fork detector for THz radiation

Ulrike Willer[1,*], Andreas Pohlkötter[1], Wolfgang Schade[1], Jihua Xu[2], Tonia Losco[2], Richard P. Green[2], Alessandro Tredicucci[2], Harvey E. Beere[3], David A. Ritchie[3]

[1]*Clausthal University of Technology, LaserApplicationCenter, Am Stollen 19/Haus3,38640 Goslar, Germany*
[2]*Laboratorio NEST, CNR-INFM and Scuola Normale Superiore, Piazza dei Cavalieri 7, 56126 Pisa, Italy*
[3]*Cavendish Laboratory, University of Cambridge, J J Thomson Avenue, Cambridge CB3 0HE, United Kingdom*
**u.willer@pe.tu-clausthal.de*

Abstract: THz-sensing is an emerging technology that would be advantageous for a variety of applications in industry, biology, biochemistry and security, if small and convenient to use sources and detectors would be readily available. However, most of them are bulky, complicate to operate, and need cryogenic cooling. Here we present a new detection scheme that is versatile enough to detect electro-magnetic radiation within the whole spectrum, can be easily applied to the THz-range, and operates at room temperature. The mechanism is based on the resonant excitation of a quartz tuning fork.

OCIS codes: (040.0040) Detectors; (040.2235) Far infrared or Terahertz.

References and links

1. R. Köhler, A. Tredicucci, F. Beltram, H. E. Beere, E. H. Linfield, A. G. Davies, D. A. Ritchie, R. C. Iotti, and F. Rossi, "Terahertz semiconductor-heterostructure laser," Nature **417**(6885), 156–159 (2002).
2. A. Tredicucci, and R. Köhler, "Terahertz Quantum Cascade Lasers in Intersubband Transitions in Quantum Structures," (McGraw-Hill, New York), pp. 45–105 (2006)
3. B. S. Williams, "Terahertz quantum-cascade lasers," Nat. Photonics **1**(9), 517–525 (2007).
4. E. R. Brown, K. A. McIntosh, K. B. Nichols, and C. L. Dennis, "Photomixing up to 3.8 THz in low-temperature-grown GaAs," Appl. Phys. Lett. **66**(3), 285–287 (1995).
5. M. Tani, P. Gu, M. Hyodo, K. Sakai, and T. Hidaka, "Generation of coherent terahertz radiation by photomixing of dual-mode lasers," Opt. Quantum Electron. **32**(4/5), 503–520 (2000).
6. N. Chimot, J. Mangeney, P. Crozat, J. M. Lourtioz, K. Blary, J. F. Lampin, G. Mouret, D. Bigourd, and E. Fertein, "Photomixing at 1.55 μm in ion-irradiated In(0.53)Ga(0.47)As on InP," Opt. Express **14**(5), 1856–1861 (2006).
7. A. J. Kreisler, and A. Gaugue, "Recent progress in high-temperature superconductor bolometric detectors: from the mid-infrared to the far-infrared (THz) range," Supercond. Sci. Technol. **13**(8), 1235–1245 (2000).
8. P. Lebedew, "Untersuchungen über die Druckkräfte des Lichtes," Ann. Phys. **311**(11), 433–458 (1901).
9. E. F. Nichols, and G. F. Hull, "Über Strahlungsdruck," Ann. Phys. **317**(10), 225–263 (1903).
10. K. Karrai, and R. D. Grober, "Piezoelectric tip-sample distance control for near field optical microscopes," Appl. Phys. Lett. **66**(14), 1842–1844 (1995).
11. F. J. Giessibl, "Atomic resolution on Si(111)-(7x7) by noncontact atomic force microscopy with a force sensor based on quartz tuning fork," Appl. Phys. Lett. **76**(11), 1470–1472 (2000).
16. A. Pohlkötter, U. Willer, C. Bauer, and W. Schade, "Resonant tuning fork detector for electromagnetic radiation," Appl. Opt. **48**(4), B119–B125 (2009).
12. T. Losco, J. Xu, R. P. Green, A. Tredicucci, H. E. Beere, and D. A. Ritchie, "THz quantum cascade designs for optimized injection," Physica E **40**(6), 2207–2209 (2008).
13. J.-M. Friedt, and É. Carry, "Introduction to the quartz tuning fork," Am. J. Phys. **75**(5), 415–422 (2007).
14. X. Jun, Y. Bo, L. Xin, and C. Juan, "Theoretical model and optimization of a novel temperature sensor based on quartz tuning fork resonators," Phys. Scr. **T 129**, 316–320 (2007).
15. A. A. Kosterev, Y. A. Bakhirkin, and F. K. Tittel, "Ultrasensitive gas detection by quartz-enhanced photoacoustic spectroscopy in the fundamental molecular absorption bands region," Appl. Phys. B **80**(1), 133–138 (2005).
16. A. Pohlkötter, U. Willer, C. Bauer, and W. Schade, "Resonant tuning fork detector for electromagnetic radiation," Appl. Opt. **48**(4), B119–B125 (2009).

1. Introduction

The lack of small and easy to operate THz sources and detectors hinders the large scale introduction of THz technology into industrial process control as well as into biological, biochemical and security applications. Several sensitive lab-based generation and detection

#113258 - $15.00 USD Received 23 Jun 2009; revised 23 Jul 2009; accepted 23 Jul 2009; published 29 Jul 2009

schemes exist, e.g. the use of coherent techniques. However, progress in miniaturization has mainly been made on the side of THz sources: quantum cascade lasers (QCL) [1–3] and photomixers [4–6] are systems that have the potential to become portable devices. Detection, however, is still difficult: either low temperature devices are needed, e.g. Si-bolometers, that guarantee a high sensitivity, or detectors that were actually developed for other spectral regions and present a residual sensitivity in the THz range are often used. A drawback of the latter is that background radiation at the original design wavelength is detected much more efficiently than the terahertz radiation. Considerable advances have been achieved with various bolometric detection schemes; nevertheless, a state of technological maturity has not yet been reached [7]. In this contribution a new approach for detecting electromagnetic radiation is described and its applicability to the THz range is demonstrated. The operating principle is based on the resonant excitation of a mechanical oscillator by an electromagnetic wave. A linear behavior between power and derived signal is found for constant pulse width of the QCL source employed. This room temperature device can serve as a low-cost detector in many THz sensing systems.

2. Theoretical background

Radiation pressure, i.e. the pressure caused by the electromagnetic radiation incident on a surface, was first experimentally observed by Lebedew [8] and Nichols and Hull [9]; it can be described as due to the transfer of momentum from the incident photons to the material. To enhance the effect, one can employ a resonant system, for instance in the form of a tuning fork (TF). The deflection of the TF due to transfer of photon-momentum from the electro-magnetic radiation to the mechanical oscillator is greatest when the illuminating photon flux is modulated at the resonance frequency of the oscillator. This results in a periodic force driving the TF into oscillation. The force $\vec{F}$ applied to the surface by a flux Φ of n photons per unit time across a unit area is given by the transfer of momentum:

$$\vec{F} = \Phi \cdot \delta \vec{p} = \Phi \eta \cdot \frac{hf}{c} \cdot \hat{i} = \frac{\eta}{c} \cdot \vec{P} \cdot \tag{1}$$

Here $\vec{P}$ is the Poynting vector of the incident radiation, hf the photon energy, h the Planck constant, c the velocity of light and $\hat{i}$ the unit vector lying along the propagation direction of the electromagnetic wave. The factor η differs for absorption ($\eta = 1$) and reflection ($\eta = 2$).

As the amplitude of a driven harmonic oscillator is proportional to that of the driving force, the amplitude of the oscillator is directly proportional to the amplitude of the modulated electro-magnetic radiation. The oscillation of a quartz TF can easily be determined via the piezoelectric effect. Bending of the prongs gives rise to a piezo current which can be amplified and measured. Thus, an alternating electrical signal directly proportional to the optical power is produced by the tuning fork. A mathematical description with the differential equation of the driven harmonic oscillator is then possible:

$$x(t)\,\omega^2 + \gamma\,\dot{x}(t) + \ddot{x}(t) = \frac{1}{m} F(t) \cdot \tag{2}$$

Here, x is the deflection of the harmonic oscillator; γ is the damping factor and $\omega^2 = k/m$ is the square of the angular frequency with k being Hooke's constant and m the mass of the oscillator. If the radiation is modulated in the form of a rectangular function, the differential equation for the driven harmonic oscillator can be treated by expanding the driving force into a Fourier series:

$$F(t) = A \cdot \left(\Omega \cdot \tau + \sum_{j=1}^{\infty} \frac{2}{j \cdot \pi} \sin\left(j \cdot \pi \cdot \tau \cdot \Omega\right) \cos\left(2\pi \cdot \Omega \cdot \left(t - \frac{1}{2\Omega}\right) \cdot j\right) \right). \tag{3}$$

Here, A is the amplitude of the driving force, Ω its frequency and τ measures the width of one rectangular pulse. The time origin is chosen so that the first pulse is centered around $t = 1/(2\Omega)$. In the following calculations, only the first 40 summands are considered within the differential equation. As resonance frequency of the tuning fork ω and frequency of

#113258 - $15.00 USD Received 23 Jun 2009; revised 23 Jul 2009; accepted 23 Jul 2009; published 29 Jul 2009

the driving force Ω the same value 32760 Hz is used. The damping coefficient can be determined from the quality factor of the TF: for Q = 54000 we use $\gamma = 3.81*10^{-6}\ \mu s^{-1}$, which corresponds to our experimental conditions. The amplitude of the driving force can be determined by use of Eq. (1), assuming reflection of the radiation ($\eta = 2$), which is justified because of the metallic coating, serving as an electrode, which covers the TF prong. The mass of the TF is determined from the geometric properties and the density of quartz. Hooke's constant $k = E\ w\ t^3/(4L^3)$ can be calculated from the geometrical properties of the TF and Young's modulus of quartz $E = 7.87*10^{10}\ N/m^2$ [10]. With the length of one prong L = 3.8mm, its thickness t = 590µm and its width w = 250µm the static spring constant is calculated to be $k = 1.84*10^4$ N/m. With these parameters the deflection of the TF is simulated for an incident cw power of 1W. Figure 1a shows the result on a millisecond scale where the buildup of the oscillation is clearly visible, whereas Fig. 1b shows an arbitrarily chosen interval on the µs scale to show the driven oscillation itself.

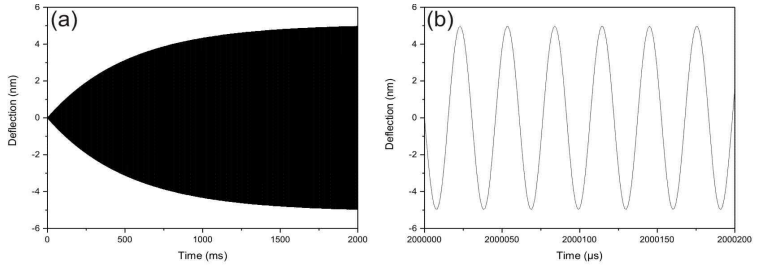

Fig. 1. Simulation of the deflection of one prong of the tuning fork: a) buildup of the oscillation, b) forced oscillation for driving of the tuning fork with a quasi cw power of P = 1W.

The deflection of the quartz TF gives rise to a piezo current. The current per deflection generated by the TF is given by Giessibl [11]. With the piezo-electric coupling coefficient $d_{12} = 2.31\ 10^{-12}$ C/N [10] and the geometric properties given above, a current per deflection of 4.4 A/m is generated by the used TF. With a 10 MΩ resistor of the transimpedance amplifier, signals of tens of µV are generated for deflections on the pm scale.

Fig. 2. Calculated deflection per W of incident quasi cw power as function of the pulse width of the driving electromagnetic wave.

To map out the dependence on pulse width, $x(t)$ is determined for different values of τ. In this case, it is important to distinguish between the influence of increased quasi cw power due to longer pulse width at the same amplitude and the efficiency of driving the oscillator with varying pulse widths. In the experiment this can be done by dividing the results obtained with the new detector by the reference measurement with a bolometer or Golay cell for the different pulse widths. In the calculation, the quasi cw power was fixed at constant repetition rate resulting in different peak powers for the varying pulse width. Figure 2 shows the calculated values for the generated deflection while driving the TF with different pulse widths. The differential deflection $x(t)_{max} - x(t)_{min}$ has been obtained for different pulse width and fixed quasi cw power (P = 1W), i.e. fixed incident momentum. It can be seen, that the oscillator is driven most effectively with short pulses.

#113258 - $15.00 USD Received 23 Jun 2009; revised 23 Jul 2009; accepted 23 Jul 2009; published 29 Jul 2009

3. Experimental

A quantum cascade laser is used as the THz source. It employs a strongly diagonal bound-to-continuum design operating at 2.8 THz with a low-loss waveguide relying also on the metal layer below the substrate for optical confinement [12]. The laser is mounted within a cryostat and cooled down to around T = 10 - 20 K for operation. The driver is triggered to generate rectangular pulses of variable width with a repetition rate of RR = 32760 Hz. For comparison, measurements are also performed with a silicon bolometer and a Golay cell. To do so, the rapidly modulated radiation (32 kHz) is additionally gated with a rectangular function at 310 Hz for the bolometer or 13 Hz for the Golay cell. The THz radiation is collimated with an off-axis parabolic mirror with f = 15 cm focal length, guided via a flat mirror over a distance of about 120 cm and then focused onto the detector device with a second off-axis parabolic mirror with f = 10 cm as shown in the schematic of the experimental setup in Fig. 3. For the images an intermediate focus was generated by two additional parabolic mirrors (f = 5 cm and f = 10 cm). For the detector we employ a commercially available quartz TF. These oscillators are designed for use within watches but have also been used extensively for example for distance control of scanning microscopes [10,13], as temperature sensors [14] and for gas detection with quartz enhanced photoacoustic spectroscopy (QEPAS) [15]. For use as a detector, the housing is removed so that the prongs are easily accessible. The TF is mounted within a small cell that can be evacuated to minimize damping effects of surrounding gas molecules, with the radiation being transmitted through a polyethylene window and focused onto the side of one prong. The oscillation of the TF is measured via the piezoelectric effect. The generated current is amplified with a transimpedance amplifier with a 10 MΩ feedback resistor, and the signal is subsequently processed with a lock-in amplifier.

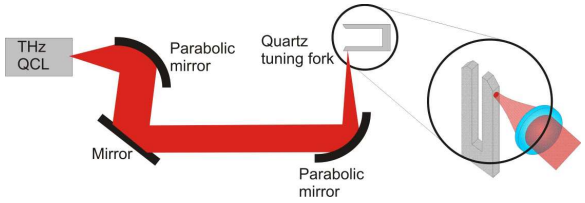

Fig. 3. Schematic of the experimental setup.

4. Results

For a detector a linear response characteristic between incident power and output signal is of the greatest importance. Therefore, measurements are performed with different power settings of the laser. The influence of the pulse width is also determined and compared with theory.

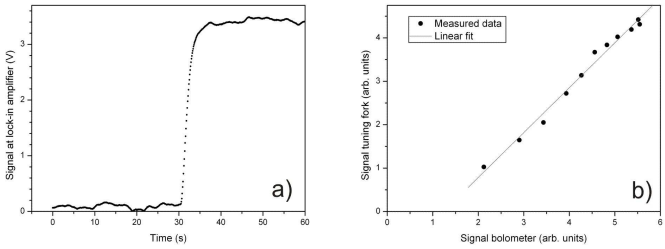

Fig. 4. (a) Signal of the photon momentum detector while the THz radiation is only incident in the second 30s and initially blocked; (b). Linear power characteristics of the photon momentum detector.

Figure 4a shows a typical measurement with the TF detector where the THz radiation is blocked for t = 30 s and then for the next 30 s radiation is incident on its surface. The lock-in amplifier is set to a time constant of τ = 300 ms and the QCL is driven at a current density of about 150 A/cm^2, for which the emitted quasi cw power is measured to be of the order of 0.5

#113258 - $15.00 USD Received 23 Jun 2009; revised 23 Jul 2009; accepted 23 Jul 2009; published 29 Jul 2009

mW. The detector response time is mainly determined by the quality factor of the resonator and is in the range of several hundred milliseconds which corresponds well with calculated values. The background level is determined by the thermal movement of the prongs of the TF. Careful electromagnetic shielding is necessary; otherwise, a comparatively high background level is induced due to sensitivity to electronic crosstalk between the tuning fork, connecting cables, and the amplifier, which act like antennas, and the laser driver and connecting cables. Similar measurements performed with a time constant of τ = 100 ms with the radiation incident for 5 seconds and then blocked for 5 seconds at different laser drive currents were performed as function of incident laser power. Owing to the presence of some crosstalk between electronics and tuning fork, the difference of the values measured with incident radiation and blocked radiation is referred to as the real signal of the photon momentum detector. As the laser power increases nonlinearly with applied voltage, it was monitored with a bolometer and then these values were used for characterizing the photon momentum detector. Figure 4b shows the resultant signal of the photon momentum detector as function of the power of the THz radiation. A linear dependence is clearly visible. The crosstalk does not affect the linearity of the detector, since the difference in phases is constant, but prevents zero crossing, as can be observed in Fig. 4b. Since the signal depends on the characteristics of the tuning fork (quality factor) as well as on the position of the focus, calibration has to be done with each single device and the slope is not conferrable between measurements after realignment.

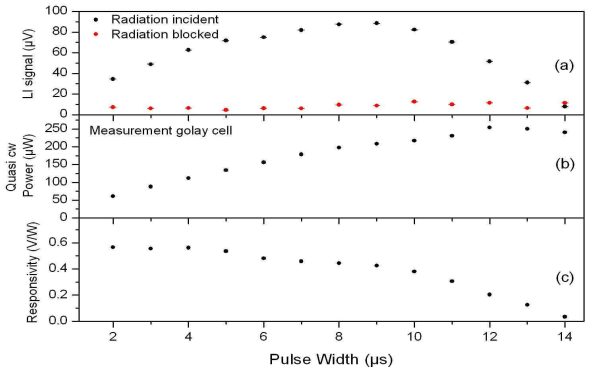

Fig. 5. Dependence of the tuning fork detector signal on pulse width: (a) measured signal and background data for different pulse widths, (b) quasi cw power measured with a Golay cell, (c) calculated responsivity of the tuning fork detector.

The crosstalk can be further reduced by a different orientation of the cryostat with respect to the tuning fork. With this setup the dependence on the pulse width was investigated. The temporal behavior of the driving force (i.e. in this case the pulse duration) has great influence on the signal. To map out this influence, measurements are performed with the same voltage settings at the driver but different pulse lengths varying between 1 µs and 14 µs. The radiation was blocked for t = 30 s and was subsequently incident for 30 s. In both time frames the signal is determined by a numerical fit of a constant and then added to Fig. 5a. It has to be noted, that the background signal is independent from the pulse width, indicating that the crosstalk has been successfully suppressed. The remaining noise floor is due to the thermal movement of the prongs. The dependence of the signal on the pulse length, as simulated in Fig. 2, is, however, masked by the varying optical quasi cw power that is incident on the TF. Therefore, measurements have been performed also with a Golay cell for the same settings. With a responsivity of 2903.5 V/W for 13 Hz modulation at 2.8 THz of the Golay cell, the incident quasi cw power has been determined (refer to Fig. 5b). The responsivity of the detector device can then be determined by dividing the measured signal by the incident power, and is given in Fig. 5c. As theory predicts, driving of the oscillator is most efficient with short pulses. A comparison with Fig. 2 shows good correspondence. The specific detectivity of the sensor has been determined by noise analysis in the visible and mid-infrared spectral region (MIR) and a

#113258 - $15.00 USD Received 23 Jun 2009; revised 23 Jul 2009; accepted 23 Jul 2009; published 29 Jul 2009

value of D* = 10^5 cm $Hz^{1/2}$/W has been found [16]. The detector has been tested with visible and MIR radiation as well. In contrast to the here presented results for THz-radiation, much higher values than expected from the transfer of momentum have been measured for these spectral regions [16]. Thus, in the visible and MIR, the effect cannot be attributed solely to the transfer of photon momentum. Even though the here measured values correspond well with the deflections expected from the force due to transfer of momentum alone, we do not conclude that this is the only acting force: Due to the different sensor area for Golay cell and TF detector, the radiation measured with the Golay cell might not have been concentrated totally on the TF so that, also in the THz-range, signals higher than expected might have been measured. Future investigations need to clarify if a second force is acting on the TF while irradiated with modulated electro magnetic radiation. The generated signal is proportional to the quasi cw power incident on the TF. In practical applications, the peak power is often confined to a specific value and the quasi cw power is increased by either modifying the modulation frequency or using longer pulses. Since for a given tuning fork the pulse repetition rate is fixed at its resonance frequency and cannot be changed, a trade off between the increase of quasi cw power and efficient driving of the oscillator has to be found. In this case, the maximum signal was obtained at a pulse duration of τ = 8µs. The detector has finally been used for imaging of different samples. The samples were mounted on a x-y stage and scanned through the intermediate focus generated by a parabolic mirror with f = 5 cm focal length. The beam spot at this plane was measured to be 0.5 mm in diameter. Figure 6 shows images of an aluminum foil with cut out letters: Fig. 6a is a reference image taken with the Golay cell, whereas Fig. 6b shows the measurement with the tuning fork detector. The resolution for both images is restricted by the step size for the scanning and is 1 mm in each direction. As second sample leafs were taken as shown in Fig. 6c, which displays a photograph, while Fig. 6d shows the THz image with a resolution of 0.5 mm in each direction. It can be clearly seen that not only the outline of the leaves is measurable but also inner structures of the bigger leaf: part of it has already dried while other sections are nearly opaque due to high water content.

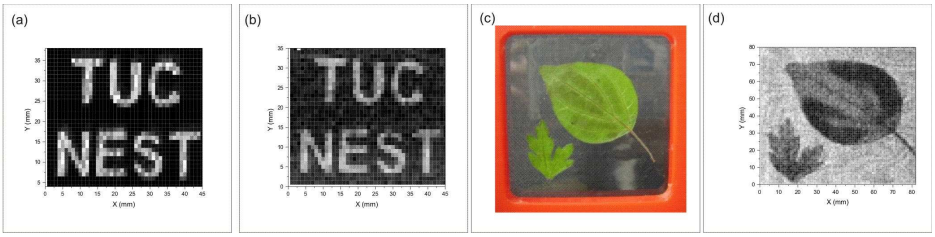

Fig. 6. Scanned images of a sample of aluminum foil with cut out letters and leaves: (a) taken with Golay cell, (b) taken with TF detector, (c) photograph, (d) taken with TF detector.

5. Conclusions

The photon momentum detector is a versatile new device for sensing of THz radiation. The power characteristic is linear for constant pulse duration and fixed pulse shape. The detection limit depends on the pulse width. For τ = 8 µs a limit of P = 50 µW quasi-cw power was found. Although its specific detectivity is at present 3 orders of magnitude worse than that of pyroelectric detectors, it has a great potential for sensing applications in the THz range, esp. when combined with THz-QCLs. Since it is low in cost, small in size and works at room temperature, it could be integrated into the QCL housing as a monitor detector similar to photo diodes in laser diodes. Improvements in sensitivity and detectivity can be reached with better evacuation and focusing and the use of the optimal pulsewidth.

#113258 - $15.00 USD Received 23 Jun 2009; revised 23 Jul 2009; accepted 23 Jul 2009; published 29 Jul 2009